

# Correcting for interference effects in the photoluminescence of Cu(In,Ga)Se<sub>2</sub> thin films

Max Hilaire Wolter<sup>\*1</sup>, Benjamin Bissig<sup>2</sup>, Patrick Reinhard<sup>2</sup>, Stephan Buecheler<sup>2</sup>, Philip Jackson<sup>3</sup>, and Susanne Siebentritt<sup>1</sup>

<sup>1</sup> Laboratory for Photovoltaics, Physics and Materials Science Research Unit, University of Luxembourg, 4422 Belvaux, Luxembourg

<sup>2</sup> Laboratory for Thin Films and Photovoltaics, Empa – Swiss Federal Laboratories for Materials Science and Technology, Überlandstr. 129, 8600 Dübendorf, Switzerland

<sup>3</sup> Zentrum für Sonnenenergie- und Wasserstoff-Forschung Baden-Württemberg (ZSW), 70565 Stuttgart, Germany

Received 31 August 2016, accepted 30 January 2017

Published online 21 February 2017

**Keywords** Cu(In,Ga)Se<sub>2</sub>, interference, photoluminescence, thin films

\* Corresponding author: e-mail max.wolter@uni.lu, Phone: +352 46 66 44 5191, Fax: +352 46 66 44 35191

Photoluminescence (PL) measurements are performed on high-quality Cu(In,Ga)Se<sub>2</sub> (CIGS) thin films with the intention of investigating their electronic structure. Due to the nature of the CIGS absorbers, notably their smooth surface and a graded band gap, the measured PL spectra are distorted by interference effects, limiting thus the information that one can gain. Here we show that, by varying the entrance angle of the laser light and the

detection angle of the emitted PL, we are able to correct for interference effects. As a result, we receive interference-free PL spectra that enable us to determine quantities such as band gap energies and quasi-Fermi level splittings (QFLS). Furthermore, we show that it is possible to measure the QFLS even without correcting for interference effects and we compare the QFLS to the open circuit voltage for a particular sample.

© 2017 WILEY-VCH Verlag GmbH & Co. KGaA, Weinheim

**1 Introduction** Thin film solar cells based on the polycrystalline chalcopyrite Cu(In,Ga)Se<sub>2</sub> (CIGS) recently reached an efficiency of 22.6% on rigid [1] and 20.4% on flexible substrates [2] getting thus ever closer to the 25.6% [3] efficiency currently held by the market dominating silicon-based solar cells. In order to further improve the efficiency of CIGS-based solar cells by identifying and eliminating potential device limitations, there is a need for a better understanding of the material properties of their thin film absorbers. A versatile method to investigate the electronic structure such as defects [4–6], potential fluctuations [7, 8], or quasi-Fermi level splittings [9, 10], is photoluminescence (PL). This method is based on the radiative recombination of photo-generated charge carriers following laser illumination. PL measurements carried out at room temperature on CIGS absorbers generally yield spectra that consist of a single peak [11]. However, depending on the nature of the absorbers, particularly the presence of a double gallium gradient and a smooth surface as is the case in state of the art high quality absorbers, interference effects may occur and disturb the

measured spectra [12, 13]. The distortion results in several peaks or shoulders that would otherwise not have formed. Alternatively, a PL spectrum showing several peaks can hint at the presence of additional phases, such as ZnSe in the Cu<sub>2</sub>ZnSnSe<sub>4</sub>-based thin film [14]. Hence, it is essential to distinguish between real peaks and peaks caused by interference effects. Given that interference effects severely limit the information that can be gained from PL, there is a need to correct for them.

In this study, we introduce a new solution by showing that it is possible to remove the interference effects that affect the spectra by measuring the PL for a multitude of varying entrance and detection angles. Additionally, we measure the quasi-Fermi level splitting (QFLS) by absolute calibrated PL and show that its value can be determined even in the presence of interference effects.

**2 Background** In PL experiments, photons emitted from a recombination center inside the semiconducting thin film can travel back and forth through the layer before exiting and being collected by a detector. This process is

schematically depicted in Fig. 1a. Depending on their phase, the exiting photons can interfere constructively or destructively, resulting in the observed interference pattern in the measured spectra. However, as is described in the recent study by Larsen et al. [13], the interference pattern is not observed unless a series of requirements are met. These include that the sample surface must be sufficiently smooth, that the reflectance at the back must be high, that the film thickness must be such that the spectral distance between the interference fringes is similar to the width of the PL signal, and that the emitted photons must only be weakly absorbed on their way through the layer. Given these conditions, a high-quality CIGS absorber with a smooth surface and a double gallium gradient [15] is likely to exhibit interference effects as its PL is predominantly emitted from the introduced band gap minimum. In order to verify if the PL signal is affected by interference effects, it is possible to compare it with the reflectance spectrum of the absorber under investigation. This procedure is briefly explained in the supplementary material.

Approaching the interference problem in a simple manner, we can assume that the interference fringes mimic Fabry–Perot oscillations and can be described by an Airy function [16]. The Airy function depends on the optical path length of the involved waves i.e., the phase difference they collect inside the material. A change of the optical path length then leads to a shift of the interference fringes in the PL spectra. This shift can be measured in angle-resolved photoluminescence (ARPL) experiments by tilting the sample by an angle  $\theta$  and collecting the photons that travel a different path through the layer, as is depicted in Fig. 1b.

**3 Experimental** The samples we use consist of approximately  $2.5\ \mu\text{m}$  thin CIGS absorbers grown in a

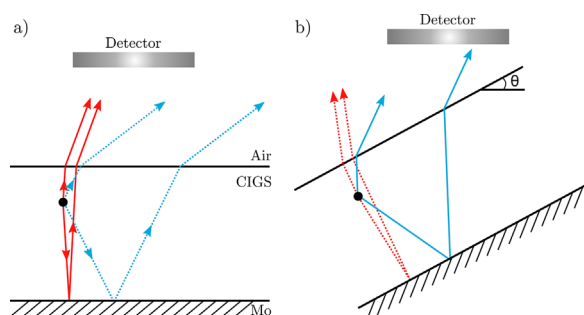


**Figure 1** Schematic depiction of two PL measurement configurations where two possible photon paths inside a CIGS absorber grown on molybdenum are shown. The black dot represents the recombination center that emits the PL. The detector remains stationary. (a) In normal configuration, only the photons that are emitted close to perpendicular to the interface between the absorber and air (straight red lines), can be detected. Photons emitted in other directions (dotted blue lines) cannot be detected in this configuration. (b) By tilting the sample by an angle  $\theta$ , it is possible to collect the previously unattainable photons (straight blue lines) while the previously collected photons (dotted red lines) are now out of detector range.

multi-stage co-evaporation process on molybdenum-coated soda lime glass and received several alkaline post-deposition treatments [1, 2]. The corresponding finished solar cells show efficiencies of 20%. Angle-resolved photoluminescence experiments are carried out both intensity calibrated and uncalibrated.

**3.1 Angle-resolved photoluminescence** In the intensity uncalibrated photoluminescence experiments, the absorbers are excited by a photon flux of approximately  $10^{22}$  photons  $\text{cm}^{-2}\text{s}^{-1}$  on a spot size of approximately 2 mm diameter from an Ar<sup>+</sup> laser with a wavelength of 514.5 nm. In the intensity calibrated photoluminescence experiments done to determine the absolute value of the QFLS, the excitation source is the 660 nm line of a diode laser while the photon flux is set to  $2.1 \cdot 10^{21}$  photons  $\text{cm}^{-2}\text{s}^{-1}$  on a 1.8 mm diameter spot size equaling the photon flux of the AM 1.5 sun spectrum above the assumed band gap of 1.1 eV. In both cases, the emitted photoluminescence is collected ( $f/\#$  of 2) by off-axis parabolic UV-enhanced aluminum mirrors and fed into a spectrometer with 303 mm focal length where it is spectrally dispersed and detected by a 512 element InGaAs array. All measurements are carried out at room temperature and are spectrally corrected using a commercial calibrated halogen lamp.

The sample is mounted onto a rotary disc platform and fixed in such a way that its surface lies exactly on the rotation axis. This placement ensures that the laser spot remains on the same position on the sample surface, even for large tilting angles. A schematic depiction is provided in Fig. 2. The experiment is initiated by measuring the photoluminescence after excitation normal to the surface. Afterwards the sample is rotated by consecutive angles  $\theta$  and its PL measured for each angular step. We choose to measure the PL for angles between 0 and  $75^\circ$  in intervals of  $5^\circ$ .

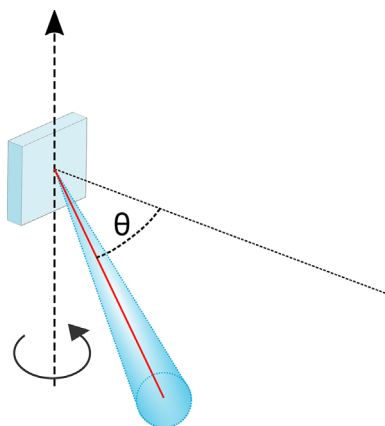


**Figure 2** Schematic depiction of the sample placement for ARPL experiments. The sample surface lies exactly on the rotation axis. Tilting the sample by an angle  $\theta$  results in an angular change of the excitation (red straight line) and collection (blue cone) direction compared to the surface normal (black-dashed line).

**3.2 Correcting for interference effects** The result of the ARPL measurement can be seen in Fig. 3. The spectra show that the interference fringes are shifting with increasing angles, indicating that we are indeed able to measure photons with different optical path lengths. Furthermore, the PL intensities of the spectra are decreasing with increasing angles. This decrease in intensity can be attributed to two reasons. Firstly, the rotation leads to an elliptic distortion of the circular laser spot on the sample. This results in a reduction of the excitation density on the absorber surface by a factor of  $\cos\theta$ . Secondly, assuming the absorber surface to be of Lambertian nature, the loss of the collected light with increasing angles can be quantified by a factor of  $\cos\theta$  as well. The proof that the PL intensity decreases with  $\cos^2\theta$  is provided in Fig. S2 in the supplementary material.

By measuring the PL for a multitude of angles, we are able to measure all the different interference fringes that affect our spectra. This means that the interference fringes are gradually shifting from a maximum into a minimum. By adding up all the angle-resolved PL spectra, the interference effects will cancel out. However, before doing so, we need to compensate for the decrease in PL intensity otherwise the PL spectra measured at large angles will not significantly contribute to the sum. By multiplying the spectra by  $\cos^{-2}\theta$ , it is possible to scale all the PL spectra to a similar intensity. The spectra can then be added up and averaged over their count. As is shown in Fig. 4, as a final result, we receive a corrected PL signal that is completely free of interference and overlays the interference riddled peak almost perfectly.

**4 Results and discussion** The corrected PL spectrum in Fig. 4 was extracted from PL spectra taken at 16 different angles up to  $75^\circ$ . Theoretically, if we would measure the PL for all tilting angles between 0 and  $90^\circ$ , we

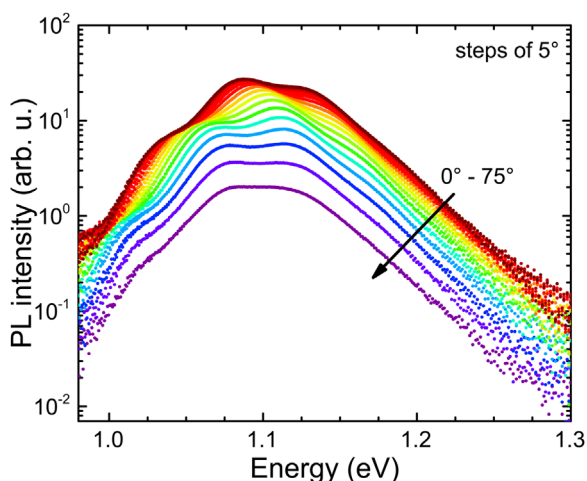


**Figure 3** PL spectra of a CIGS absorber measured for angles between 0 and  $75^\circ$  in intervals of  $5^\circ$  in logarithmic representation. The spectra show that the interference fringes are shifting with increasing angles. Furthermore, the PL intensity is decreasing with increasing angle  $\theta$ , following a  $\cos^2\theta$  dependence.

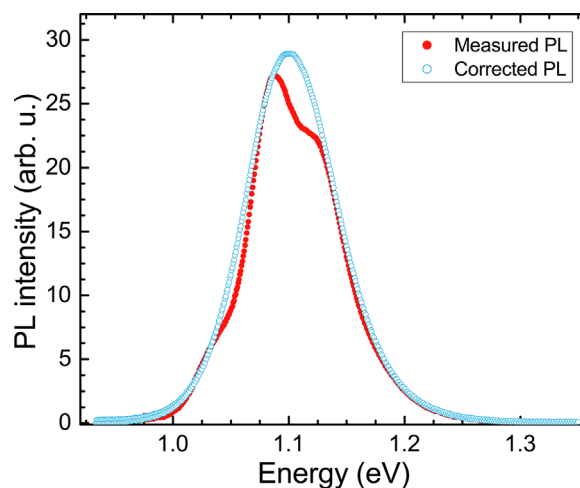


**Figure 4** Measured (filled red circles) and corrected (open blue circles) PL spectra of a CIGS absorber. The corrected PL signal is free of interference effects and overlays the measured spectrum at  $0^\circ$  perfectly.

would be able to collect the photons with all possible phases. Experimentally this is not feasible, especially for angles approaching and including  $90^\circ$ . However, as an increase of the tilting angle leads to an increase in the optical path length, the photons are running more and more out of phase and the severity of the interference effects is diminished. Hence, the photons collected at large angles are contributing less to the final sum of the spectra and can be ignored.

Furthermore, one could imagine that it would suffice to measure the PL spectra at only two different angles where the interference fringes have shifted from a maximum at one angle into a minimum at a different angle, thus dramatically decreasing the measurement time. This process would, however, not eliminate all the interference effects as the fringes are not spectrally equidistant. The different spectral distances between the fringes result from the fact that the optical constants of the thin film are dependent on the wavelength of the emitted photons and the fact that the measured PL spectra span over a rather large spectral distance of several hundred nanometers (e.g., approximately 430 nm in our case).

As our procedure example in Fig. 4 reveals, the spectra of the measured and corrected PL seem to be identical at high energies. To verify this, we measure intensity calibrated ARPL on both the bare CIGS absorber shown in Fig. 4 and on the same absorber but with a 50 nm cadmium sulfide layer on top. We then compare the quasi-Fermi level splitting of both the measured and corrected spectra. The method used to determine the QFLS is adapted from Ref. [11] and its result is shown in Fig. 5 for both samples. If evaluated at sufficiently high energies, the QFLS is identical for both the uncorrected and corrected spectra. As the QFLS represents an upper limit for the open circuit voltage  $V_{OC}$  [11, 17], it is a very useful quantity since it serves to gauge the potential efficiency without finishing the solar cell. In the case of the high-quality CIGS with CdS

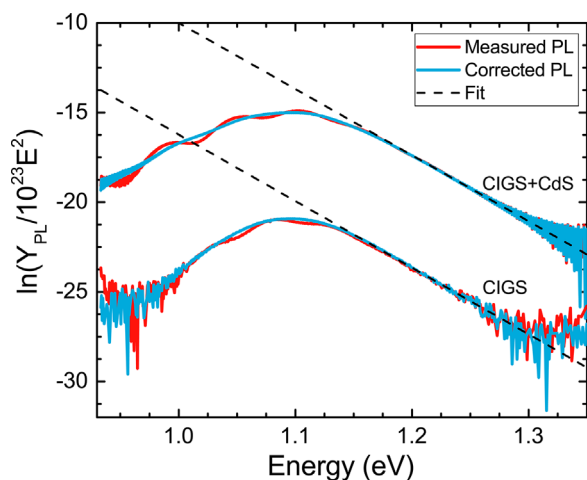


**Figure 5** Graph showing the extraction of the quasi-Fermi level splitting from both the uncorrected and corrected intensity calibrated PL spectra of a bare CIGS (lower spectra) and a CIGS + CdS (upper spectra) absorber. A QFLS fit at high energies reveals an identical value for both corrected and uncorrected spectra of 563 meV for the bare CIGS absorber and 729 meV for the CIGS + CdS absorber. The considerably smaller QFLS of the bare CIGS absorber is due to the degradation of its surface.

absorber, the QFLS amounts to 729 meV. IV measurements carried out on the corresponding solar cell reveal a  $V_{OC}$  of 725.5 mV, indicating that the loss in potential  $V_{OC}$  from the absorber to the finished solar cell is vanishingly small.

Consequently, angle-resolved photoluminescence is an easy and quick method to measure interference-free PL spectra and extract valuable information, such as the peak position, from otherwise interference distorted spectra. Additionally, the method is purely experimental which means that no assumptions concerning the optical constants are made, as is otherwise the case for models simulating the interference functions. Unfortunately, the method also presents a major drawback: should the PL spectrum shift with varying excitation density, as is generally the case at low temperatures, tilting the sample leads to a shift of the interference fringes due to both a change of the angle and a change in excitation density. In that case, the interference effects cannot be erased via ARPL.

**5 Conclusions** In high quality CIGS thin films, interference effects can be observed to negatively affect photoluminescence spectra by limiting the information that one can gain from these measurements. To verify if interference effects are indeed present, one can measure the reflectance or angle-resolved photoluminescence. The latter is a measurement method that consists of collecting the emitted photons for different excitation and detection angles at room temperature. By making use of the different optical path lengths of the collected photons, it is possible to go through the different shifts of the interference fringes and ultimately remove them. We could also show that

interference effects do not affect the high-energy side of the PL spectra, making it thus possible to extract quantities such as the quasi-Fermi level splitting even without correcting for interference.

**Supporting Information** Additional supporting information may be found in the online version of this article at the publisher's web-site.

**Acknowledgements** This work has received funding from the European Union's Horizon 2020 research and innovation programme under grant agreement no. 641004 (SharC25). This work was supported by the Swiss State Secretariat for Education, Research and Innovation (SERI) under contract number 15.0158.

## References

- [1] P. Jackson, R. Wuerz, D. Hariskos, E. Lotter, W. Witte, and M. Powalla, *Phys. Status Solidi RRL*, **10**, 583 (2016). DOI: 10.1002/pssr.201600199
- [2] A. Chirila, P. Reinhard, F. Pianezzi, P. Bloesch, A. R. Uhl, C. Fella, L. Kranz, D. Keller, C. Gretener, H. Hagendorfer, D. Jaeger, R. Erni, S. Nishiwaki, S. Buecheler, and A. N. Tiwari, *Nature Mater.*, **12**, 1107 (2013).
- [3] M. A. Green, K. Emery, Y. Hishikawa, W. Warta, and E. D. Dunlop, *Prog. Photovolt. Res. Appl.*, **23**(1), 1 (2015).
- [4] A. Bauknecht, S. Siebentritt, J. Albert, and M. C. Lux-Steiner, *J. Appl. Phys.*, **89**, 4391 (2001).
- [5] C. Spindler, D. Regesch, and S. Siebentritt, *Appl. Phys. Lett.*, **109**, 032105 (2016).
- [6] S. Siebentritt, N. Rega, A. Zajogin, and M. Ch. Lux-Steiner, *Phys. Status Solidi C*, **1**, 2304 (2004).
- [7] S. A. Schumacher, V. Alberts, and J. R. Botha, *J. Appl. Phys.*, **99**, 063508 (2006).
- [8] I. Dirnstorfer, M. Wagner, D. M. Hofmann, M. D. Lampert, F. Karg, and B. K. Meyer, *Phys. Status Solidi A*, **168**, 163 (1998).
- [9] L. Gütaý and G. H. Bauer, *Thin Solid Films*, **515**, 6212 (2007).
- [10] L. Gütaý, D. Regesch, J. K. Larsen, Y. Aida, V. Depredurand, and S. Siebentritt, *Appl. Phys. Lett.*, **99**, 151912 (2011).
- [11] T. Unold and L. Gütaý, in: *Advanced Characterization Techniques for Thin Film Solar Cells*, edited by D. Abou-Ras, T. Kirchartz, and U. Rau (Wiley-VCH, Berlin, 2001), p. 151.
- [12] R. T. Holm, S. W. McKnight, E. D. Palik, and W. Lukosz, *Appl. Opt.*, **21**, 2512 (1982).
- [13] J. K. Larsen, S.-Y. Li, J.J. S. Scragg, Y. Ren, C. Haggglund, M. D. Heinemann, S. Kretzschmar, T. Unold, and C. Platzer-Björkman, *J. Appl. Phys.*, **118**, 035307 (2015).
- [14] R. Djemour, M. Mousel, A. Redinger, L. Gütaý, A. Crossay, D. Colombara, P. J. Dale, and S. Siebentritt, *Appl. Phys. Lett.*, **102**, 222108 (2013).
- [15] P. Jackson, D. Hariskos, R. Wuerz, O. Kiowski, A. Bauer, T. M. Friedlmeier, and M. Powalla, *Phys. Status Solidi RRL*, **9**, 28 (2015).
- [16] T. Weber, H. Stolz, W. von der Osten, M. Heuken, and K. Heime, *Semicond. Sci. Technol.*, **10**, 1113 (1995).
- [17] P. Würfel, *The Physics of Solar Cells* (Wiley-VCH Verlag GmbH & Co. KGaA, Weinheim 2009).